Title: The impact of the molecular weight on the nonequilibrium glass transition dynamics of poly(phenylmethyl siloxane) in cylindrical nanopores

Author: Katarzyna Chat, Karolina Adrjanowicz

Citation style: Chat Katarzyna, Adrjanowicz Karolina. (2020). The impact of the molecular weight on the nonequilibrium glass transition dynamics of poly(phenylmethyl siloxane) in cylindrical nanopores. "The Journal of Physical Chemistry C" Vol. 124, iss. 40 (2020), s. 22321-22330, doi 10.1021/acs.jpcc.0c07053

THE JOURNAL OF PHYSICAL CHEMISTRY C

pubs.acs.org/JPCC

Article

The Impact of the Molecular Weight on the Nonequilibrium Glass Transition Dynamics of Poly(Phenylmethyl Siloxane) in Cylindrical Nanopores

Katarzyna Chat* and Karolina Adrjanowicz*

Cite This: *J. Phys. Chem. C* 2020, 124, 22321−22330

Read Online

ACCESS | Metrics & More | Article Recommendations

ABSTRACT: Changes in the glass transition dynamics caused by nanoconfinement reveal pronounced out-of-equilibrium features. Therefore, the confinement effects weaken with time. Using dielectric spectroscopy, we have investigated the impact of molecular weight on the equilibration kinetics of the studied polymer embedded within anodic aluminum oxide nanoporous templates. For our research, we have used poly(phenylmethyl siloxane) (PMPS) with low (M_w = 2530 g/mol) and high (M_w = 27,800 g/mol) molecular weight. We have found that the observed faster dynamics of the nanopore-confined systems weakens with time, and ultimately it is possible to regain the bulk-like mobility. The equilibration time increases by reducing the pore size and lowering the annealing temperature much below the glass transition temperature of the interfacial layer, $T_{g\_interface}$. The experimental data analysis has also revealed that the molecular weight of the nanopore-confined polymer influences the recovery of the bulk segmental relaxation time, τ_α. Low-molecular-weight PMPS rearrange and reach denser packing of the polymer chains with greater ease than the high-molecular-weight one. Finally, we have also demonstrated that the molecular weight affects the relationship between the time constant characterizing the equilibration kinetics and the characteristic time of viscous flow in cylindrical channels of nanometer size.

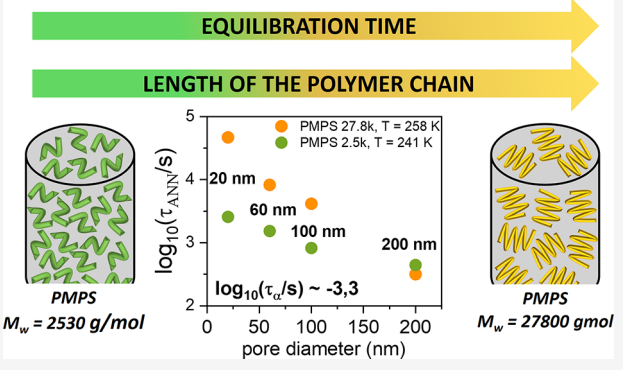

INTRODUCTION

The properties of soft matter confined at the nanoscale often differ significantly from the behavior observed for the macroscopic samples.[1−19] In recent years, numerous studies have shown that the various deviations from the bulk behavior in a confined geometry are manifestations of the nonequilibrium phenomena.[20−29] Furthermore, it has been found that prolonged annealing at temperatures above the glass transition temperature reduces or even eliminates the effects caused by the nanoconfinement.[20,24,26−30]

In the case of one-dimensional (1D) geometrical nanoconfinement, it has been observed that the many macroscopic properties can be recovered with time.[20−24] Literature data show that the faster dynamics observed for thin films of poly(methyl methacrylate) and poly(vinyl acetate) slows down during prolonged annealing.[20] It has also been found that the enhanced segmental motion in the polymer thin films of poly(4-chlorostyrene) is the nonequilibrium phenomenon.[21−24] Moreover, prolonged annealing can reduce changes in the glass transition temperature and the dielectric strength caused by confinement.[25−27,31−34] It has also been suggested that the time needed to recover the bulk properties depends on the molecular weight of the polymer system as well as the type of interaction with the substrate.[22−26] Literature results have demonstrated that the equilibration phenomena observed in thin films are associated with an increase in irreversible chain adsorption on the supporting substrate. Prolonged annealing causes changes in the conformation of the polymer chains located close to the substrate, which implies denser packing.[25−27,31−34]

Apart from thin films, nanopore-confined systems also can exhibit out-of-equilibrium features.[28,29,35−37] Numerous studies show that in the presence of two-dimensional (2D) nanoconfinement, the glass transition dynamics depends strongly on the sample's thermal history. This includes changes in the relaxation time and the glass transition temperature.[2,28,29,35−37] Furthermore, the bulk properties can be recovered with time, as reported for thin polymer films.[28,29] Importantly, in the case of confinement realized by cylindrical nanopores, the effects of annealing on glass transition dynamics are visible only in a

Received: August 1, 2020
Revised: September 10, 2020
Published: September 11, 2020

https://dx.doi.org/10.1021/acs.jpcc.0c07053
J. Phys. Chem. C 2020, 124, 22321−22330

specific temperature range, i.e., below the glass transition temperature of the interfacial layer ($T_{g\_interface}$).[28,29,35] For high-molecular-weight poly(phenylmethyl siloxane) (PMPS) confined in anodic aluminum oxide (AAO) nanopores, it has been recently shown that annealing allows recovering the bulk-like temperature dependence of the segmental relaxation time, τ_α.[28] Similar observations have been reported for the nanopore-confined epoxy resin, bisphenol-A diglycidyl ether (DGEBA).[29] Literature data demonstrate that slowing down of the confined polymer's dynamics caused by annealing is associated with changes in the polymer chain's packing density.[28,29] On the other hand, the distribution of the α-relaxation times narrows with annealing time but cannot reach that of the bulk sample.[28,29,36,37] It should also be noted that in the case of PMPS, the time needed to regain the bulk-like dynamics depends on the relative distance of the annealing temperature from the $T_{g\_interface}$ and the pore sizes.[28] From the above consideration, one can conclude that the nonequilibrium phenomena in a confined geometry have a significant impact on the soft matter's behavior at the nanoscale. Understanding how the glass transition dynamics in the macro- and nanoscale is related can provide much better possibilities for nanomaterial applications in materials sciences and various cross-disciplinary research fields.

In this work, we aim to investigate how molecular weight influences the equilibration phenomena of poly(phenylmethyl siloxane) (PMPS) under 2D nanoconfinement. For our research, we have chosen PMPS (see Figure 1) with a low

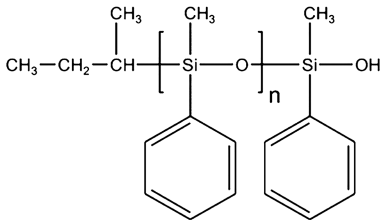

Figure 1. Chemical structure of PMPS.

molecular weight (M_w = 2530 g/mol) and compared the obtained results with that reported recently for the high molecular weight sample (M_w = 27,800 g/mol).[28] By using dielectric spectroscopy (DS), we have found out that PMPS (M_w = 2530 g/mol) confined in cylindrical nanopores also reveals prominent out-of-equilibrium features. However, the time needed to reach the equilibrium state is relatively shorter compared to the high molecular weight sample (M_w = 27,800 g/mol). Moreover, we have observed that molecular weight affects the relationship between the annealing time and the characteristic time of viscous flow in the cylindrical nanochannels. Thus, our research shows that the temperature, the size of the nanoconstraints, and also the molecular weight of the polymer can affect its nonequilibrium behavior under geometrical confinement.

EXPERIMENTAL SECTION

Materials. The tested samples are two poly(phenylmethyl siloxane) (PMPS, of different molecular weights M_w = 2530 g/mol with a polydispersity index of 1.4 (labeled as PMPS 2.5 k in the text) and M_w = 27,800 g/mol with a polydispersity index of 1.28 (labeled as PMPS 27.8 k in the text). Samples were purchased from Polymer Source Inc. and used as received. The value of the glass transition temperature, T_g, for PMPS 2.5 k and PMPS 27.8 k determined based on the dielectric relaxation study is 230 and 244.5 K, respectively.[38]

Methods. *Native Anodized Aluminum Oxide (AAO) Nanopores.* We have used AAO membranes (pore diameter of 20, 60, 100, and 200 nm, and pore depth of 100 μm) purchased from InRedox (U.S.A.). The membranes are composed of uniform hexagonal pore arrays aligned perpendicular to the surface of the material and penetrating its entire thickness. The pore channels are aligned parallel to each other. The diameter of AAO membranes is 13 mm, and their thickness 100 μm. The porosity of AAO membranes used in this study varies within 12−40%. Before infiltration, the membranes were dried at 473 K under vacuum for 24 h to remove all volatile impurities from the nanopores. Then, they were used for confining the viscous polymer. For that, a thin film of PMPS 2.5 k or PMPS 27.8 k was placed on top of each AAO membrane. Infiltration was carried out at 313 K under vacuum for 2 weeks to ensure that the material flows into the nanopores by capillary forces. After filling, the membranes were dried using a delicate dust-free tissue. Membranes were weighed before and after infiltration. The end of the filling procedure is when the mass of the confined polymer does not change with infiltration time. Based on the membrane porosity, the density of the investigated material, and the mass of the membrane before and after infiltration, it was estimated that the filling degree varies within 85−98%.

Dielectric Spectroscopy. Dielectric relaxation studies for bulk and nanopore-confined samples were carried out by using a Novocontrol Alpha analyzer. For bulk measurements of PMPS 2.5 k, we used standard plate stainless steel electrodes, separated by a Teflon spacer. Nanopore alumina membrane AAO filled with the investigated polymer were placed between two round electrodes (the diameter: 13 mm). Bulk and confined samples were measured as a function of temperature in the frequency range from 10^{-1} to 10^6 Hz. The temperature was controlled with stability better than 0.1 K using a Quatro system. Time-dependent tests were also carried out using the Novocontrol Alpha analyzer over the same frequency range, in a time step of 300 s, up to ∼2 days.

It should be noted that the dielectric data measured in this way represent a combined response of the confined polymer and loss-free alumina matrix, most likely not entirely filled with the tested material (air-gaps), where individual components have different permittivities and conductivities. Since, for the geometry under the present investigation, the electric field runs along the pore axes, the entire problem of inhomogeneous dielectrics can be modeled using series capacitances. In such a case, the dielectric permittivity of the individual components are additive, thus, $\frac{1}{\varepsilon_{por}} = \frac{1-\kappa}{\varepsilon_{sam}} + \frac{\kappa}{\varepsilon_{air}}$ where ε_{air} = 1, ε_{por} is the dielectric permittivity of the material inside the nanopores (i.e., the raw data measured using an impedance analyzer), ε_{sam} is the genuine dielectric permittivity of the confined polymer, while κ reflects the percentage of nanopores not entirely filled with the polymer. When corrected only for the porosity of the alumina membrane φ, the absolute values of ε' and the intensity of the α-relaxation process are changed in confinement ($\varepsilon'_{sam} = \frac{\varepsilon'_{por} - \varepsilon_{AAO}(1-\varphi)}{\varphi}$ and $\varepsilon''_{sam} = \varepsilon''_{por}/\varphi$). This is in line with the work by Floudas and co-workers who demonstrated that the only variable that is affected in such a case is the intensity of the dielectric signal of the confined glass-forming material, while the position of the maximum or the breadth of the α-

https://dx.doi.org/10.1021/acs.jpcc.0c07053
J. Phys. Chem. C 2020, 124, 22321−22330

relaxation peak is not affected.[39] On the other hand, incomplete filling of the pores (air gaps) acts in the same way as insulating layers. That is, it generates an additional relaxation process detected at low frequencies and shifts the α-peak to higher frequencies.[40,41] Assuming that nanopores are filled only up to 80%, we found that the shift of the α-relaxation for confined PMPS will not exceed more than 0.1 decades. In this case, changes in the distribution of the relaxation times as due to the presence of air gaps are also expected to be marginal.

RESULTS AND DISCUSSION

To investigate the equilibration kinetics of PMPS 2.5 k confined in AAO nanopores, we have carried out dielectric measurements, which involved prolonged annealing experiments at various temperatures located below the glass transition temperature of the interfacial layer. The thermal protocol used in this study includes cooling (with the rate 5 K/min) of the confined material from room temperature (T_R = 293 K) down to the desired temperature, called in the following text as the annealing temperature (T_{ANN}). Then, at the selected temperature, the time-dependent dielectric measurements were performed. In Figure 2, we demonstrate the schematic of the thermal protocol used in this experiment.

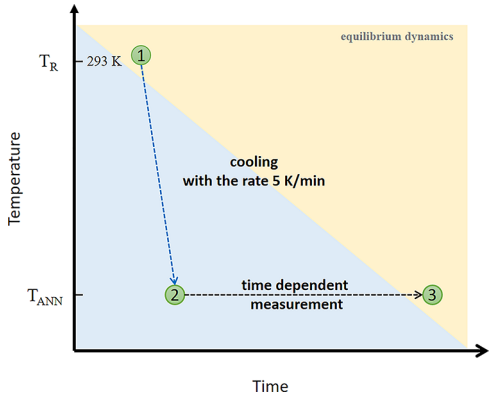

Figure 2. Schematic representation of the protocol used to record annealing. Each case starts at room temperature (1) T_R = 293 K. Then the sample is cooled at a rate of 5 K/min to the desired temperature (2) T_{ANN}. At the temperature T_{ANN}, the time measurement is carried out until the sample reaches the equilibrium state (3).

Figure 3a shows the representative time evolution of the dielectric loss spectra for the nanopore-confined PMPS 2.5 k. As shown, the maximum of the α-loss peak shifts toward lower frequencies as time passes. This observation indicates that segmental relaxation under nanopore-confinement slows down with time. In the case of the tested polymer confined in 20 nm nanopores, the equilibration process at the annealing temperature T_{ANN} = 243 K was completed after about 3.5 h. The system eventually recovered the segmental relaxation time characteristic for the bulk sample. Similar observations were also reported in the literature for glass-forming liquids and polymers confined in nanopores.[2,28,36,42,43] as well as in thin films.[20,21]

Then, to determine the characteristic relaxation time, the recorded dielectric loss spectra were fitted using the Havriliak-Negami (HN) function:[44]

$$\varepsilon^*(\varpi) = \varepsilon_\infty + \frac{\Delta\varepsilon}{[1 + (i\varpi\tau_{HN})^{\alpha_{HN}}]^{\gamma_{HN}}} \quad (1)$$

where ε_∞ is the high-frequency limit permittivity, $\Delta\varepsilon$ is the relaxation strength, τ_{HN} is the relaxation time, α_{HN} and γ_{HN} are the parameters characterizing the shape of the dielectric loss curve, and ω is the angular frequency ($\omega = 2\pi f$). Figure 3b shows the temperature dependence of the segmental relaxation time for PMPS 2.5 k in bulk and confined in 20 nm AAO nanopores. The data for the nanopore-confined samples were collected below the glass transition temperature of the interfacial layer ($T_{g\_interface} \cong 260$ K in 20 nm pores) at the initial and the final stages of the annealing process. This is because, for the nanopore-confined systems, only below the $T_{g\_interface}$, one can observe changes in the glass transition dynamics caused by the prolonged annealing.[28,29,35] As illustrated, the bulk data can be correctly described using the Vogel−Fulcher−Tammann equation (VFT).[45−47]

$$\tau_\alpha = \tau_\infty \exp\left(\frac{D_T T_0}{T - T_0}\right) \quad (2)$$

where τ_∞ is the relaxation time, T_0 is the temperature at which τ_α goes to infinity, and D_T is the fragility parameter. By analyzing the relaxation times collected at the initial stage of the annealing process, we can see that the dynamics of the nanopore-confined PMPS 2.5 k is faster compared to the bulk. This observation is consistent with the numerous studies that show the characteristic deviation of the temperature dependence of the relaxation time from the bulk behavior for the glass-forming systems confined in AAO nanopores.[1−7,42,43,48] Faster dynamics in the nanopore-confinement is related to the presence of two layers of molecules with much different mobility. The interfacial layer consists of molecules interacting with the pore walls and therefore has lower mobility. In contrast, the molecules in the core that do not interact directly with the pore walls are characterized by faster mobility. The difference in the scale of molecular movements between these two layers implies two glass transition events. In the dielectric data, the interfacial layer's glass transition temperature is typically signified as a deviation in the temperature dependence of the relaxation time from the bulk behavior.[2−6,19,43,49−51] Moreover, numerous experimental reports show that the value of the glass transition temperature of the interfacial layers determined in this case is consistent with the $T_{g\_interface}$ defined based on the calorimetric data.[2,4,10,42,52]

Importantly, we have observed that the initially faster dynamics of PMPS 2.5 k confined in 20 nm pores slow down with time. Figure 3b shows that the bulk relaxation time can indeed be recovered upon the annealing experiment. However, with decreasing annealing temperature, the time needed to reach the equilibrium state increases and exceeds the experimentally available time intervals. The slowdown of dynamics because of annealing has been reported in the literature for PMPS 27.8 k and also for the other glass-forming systems confined in AAO nanopores.[28,29] One can recall that a similar recovery of the relaxation time was reported for thin films.[20−22,24]

Next, we have focused on the changes in the distribution of the α-relaxation time upon the time-dependent experiments. In Figure 3c, we present a comparison of the normalized dielectric loss spectra for PMPS 2.5 k in bulk and confined in 20 nm AAO nanopores at the initial and final stages of annealing at T_{ANN} = 243 K. As can be seen, the distribution of the α-relaxation time narrows during annealing. However, even at the very final stage of our experiment, when the average segmental relaxation time of the bulk polymer is recovered, we still observed the

https://dx.doi.org/10.1021/acs.jpcc.0c07053
J. Phys. Chem. C 2020, 124, 22321−22330

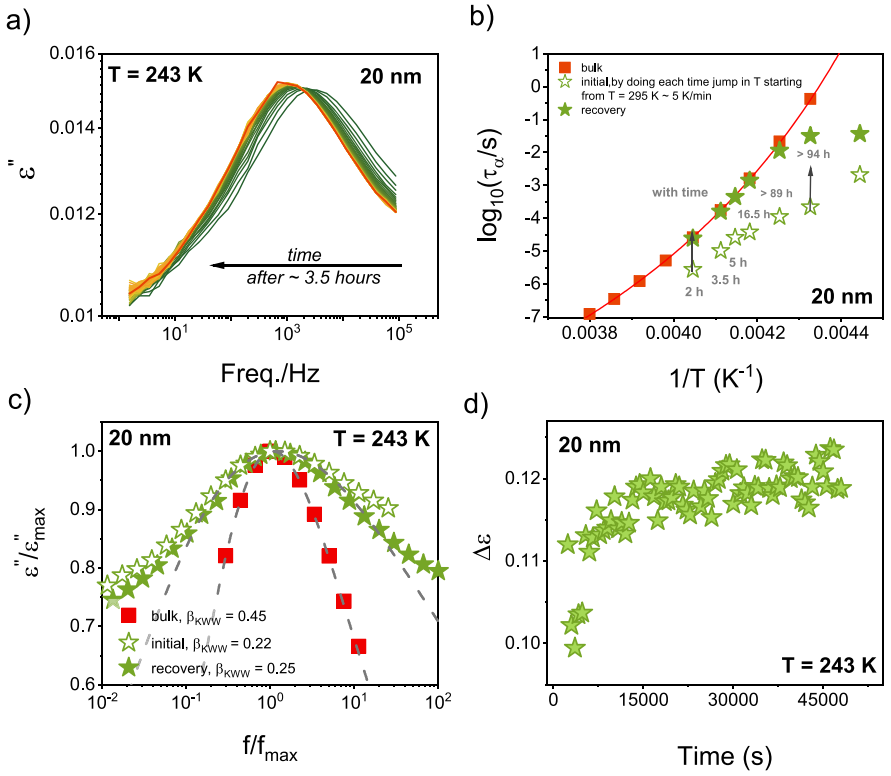

Figure 3. (a) Time-dependent changes in the dielectric loss spectra of PMPS 2.5 k confined in 20 nm AAO nanopores as measured at the annealing temperature T_{ANN} = 243 K. (b) Temperature dependence of the segmental relaxation time for PMPS 2.5 k in bulk and confined in 20 nm nanopores. The relaxation times for the confined sample were recorded after the jump from the temperature T = 295 K to the selected temperature located below $T_{g\_interface}$ (open stars) and after prolonged annealing (closed stars). The solid line is the fitting of the data to the Vogel-Fulcher-Tammann (VFT) equation. (c) Comparison of the normalized dielectric loss spectra for PMPS 2.5 k in bulk and confined in 20 nm nanopores. Confinement data were recorded before and after annealing at T_{ANN} = 243 K. Dashed lines are fits to the Kohlrausch-Williams-Watts (KWW) function. (d) Time dependence of the dielectric relaxation strength for PMPS 2.5 k confined in 20 nm nanopores measured at T_{ANN} = 243 K.

broadening of the α-loss peak. This fact indicates that the dynamics of the nanopore-confined systems remains highly heterogeneous. The narrowing of the α-relaxation peak during annealing was previously reported for PMPS 27.8 k, as well as for other glass-forming systems confined in nanopores.[28,35−37] Moreover, for PMPS 27.8 k, it has also been shown that the bulk distribution of the α-relaxation time cannot be recovered even after prolonged annealing times that enable to regain the bulk sample mobility.[28]

To describe the changes in the distribution of the segmental relaxation upon annealing, we have used the stretched exponent β_{KWW} from the Kohlrausch and Williams and Watts[53,54] function (KWW):

$$\varphi(t) = \exp\left[-\left(\frac{t}{\tau_\alpha}\right)^{\beta_{KWW}}\right] \quad (3)$$

where t is time and τ_α is relaxation time. The value of β_{KWW} varies within 0−1 and quantifies the nonexponential character of the relaxation process (β_{KWW} = 1 corresponds to the exponential power law, classical Debye-type relaxation). The narrower the width of the relaxation spectrum, the larger the value of β_{KWW}. Based on the parameters characterizing the shape of the dielectric loss spectra from the HN function, the exponent β_{KWW} can be determined: $\beta_{KWW} = (\alpha_{HN}\beta_{HN})^{1/1.23}$.[55] As shown in Figure 3c, the value of β_{KWW} increases upon the time experiment from 0.22 to 0.25, respectively, for the initial and final equilibration stage. The bulk value corresponding to that temperature is 0.45. It should be added that the narrowing of the dielectric loss peak with time has also been observed for PMPS 2.5 k confined in nanopores with different pore sizes at all considered annealing temperatures. It is worth noting that during the equilibration process in nanopores, we have also observed that the dielectric relaxation strength changes. Figure 3d shows that the $\Delta\varepsilon$ for PMPS 2.5 k increases with time. Our results are compatible with literature data for PMPS 27.8 k.[28]

To study more accurately the equilibrium recovery under the nanopore-confinement, in Figure 4a, we show the relaxation times again for PMPS 2.5 k in bulk and confined in 20 nm nanopores, recorded at the initial and final stage of annealing. These data are plotted as a function of the reduced temperature, defined as $\Delta T = T_{g\_interface} - T_{ANN}$. As observed, by increasing the distance from the glass transition temperature of the interfacial layer ($T_{g\_interface}$), the nanopore-confined system recovers mobility with bulk with much greater difficulty. In the case of the large temperature jumps (i.e., at very low annealing temperatures), we could not regain the bulk relaxation time because the time needed to reach the equilibration state exceeded our experimental time scale.

In Figure 4b, we present the changes in the segmental relaxation time for PMPS 2.5 k in AAO membranes of 20 nm pore diameter that were recorded upon prolonged annealing carried out at seven different temperatures. To describe the experimental data in a more quantitative way, we have used a stretched exponential function given as:

https://dx.doi.org/10.1021/acs.jpcc.0c07053
J. Phys. Chem. C 2020, 124, 22321−22330

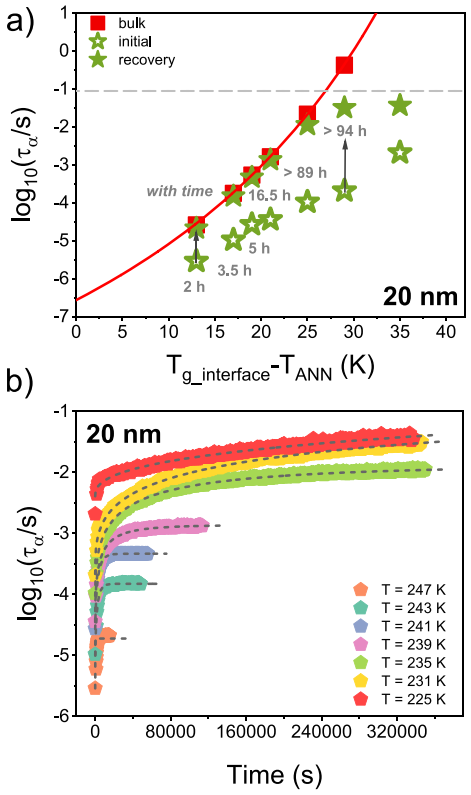

Figure 4. (a) Segmental relaxation times plotted versus the depth of annealing upon the temperature-dependent studies for the bulk PMPS 2.5 k and confined to 20 nm AAO nanopores. Data were recorded before and after annealing at seven different temperatures. Solid line is the fitting of the data to the VFT equation. (b) Changes in the α-relaxation time upon annealing of 20 nm confined PMPS 2.5 k at seven different temperatures. Dashed lines represent fits of the experimental data to the stretched exponential function.

$$\tau_\alpha = A\exp(-t/\tau_{ANN})^\beta + \tau_\infty \quad (4)$$

where τ_{ANN} is the characteristic annealing time. As shown, this approach provides a good description of the experimental data. Based on the fitting of the stretched exponential function, we have determined the characteristic annealing time constants. For PMPS 2.5 k confined in 20 nm nanopores, errors in the τ_{ANN} are around 1−4% depending on the annealing temperature. The fitting parameters for all annealing temperatures are listed in Table 1. Based on the collected data, we have found out that when decreasing the annealing temperature, the equilibration time increases.

In the next step, we have analyzed the equilibration kinetics for PMPS 2.5 k confined in AAO nanopores of different pore sizes (20, 60, 100, and 200 nm). In Figure 5, the segmental relaxation times for the bulk and the nanopore-confined samples estimated at the initial and the final stage of the annealing are plotted as a function of the reduced temperature. As demonstrated, for all pore sizes, the distance from the $T_{g\_interface}$ influences the time scale of recovery of the bulk sample dynamics. Moreover, for the smallest AAO nanopores (20 nm data shown in panel 5d) at very low temperatures, the time needed for equilibration exceeds the available experiment time. At the temperature of 231 and 225 K, the system needs more than 94 h to regain bulk mobility. On the other hand, for the 200 nm AAO nanopores (see panel 5a), the relaxation times of the bulk sample were recovered at each measured temperature,

Table 1. Fitting Parameters from the Stretched Exponential Function Describing the Equilibration Kinetics for PMPS 2.5 k Confined in 20 nm AAO Nanopores at Seven Different Temperatures of Annealing

temperature of annealing (K)	$\log_{10}(\tau_\alpha)$ initial (±0.1)	$\log_{10}(\tau_\alpha)$ final (±0.1)	stretched exponent β	$\log_{10}(\tau_{ANN})$
247	−5.5	−4.7	0.93 ± 0.03	3.12 ± 0.05
243	−5.0	−3.8	0.82 ± 0.02	3.32 ± 0.05
241	−4.6	−3.3	0.78 ± 0.01	3.41 ± 0.06
239	−4.4	−2.9	0.49 ± 0.01	3.71 ± 0.05
235	4.0	−1.7	0.44 ± 0.01	4.43 ± 0.06
231	−3.7	−0.4	0.35 ± 0.01	5.42 ± 0.45
225	−2.7	2.1	0.41 ± 0.01	7.03 ± 0.37

which suggests that reducing the pore diameter slows down the equilibration kinetics. It should be noted that for smaller pore sizes, the same bulk segmental relaxation time corresponds to a higher reduced temperature compared to nanopores with larger diameters (see Figure 5, the dashed horizontal lines indicate the same bulk value of the segmental relaxation time). As can be seen, for PMPS 2.5 k confined in 20 nm AAO nanopores, we were able to analyze data even 30 K below $T_{g\_interface}$, while for pores with a 200 nm pore diameter, it was about 17 K below the $T_{g\_interface}$. This is because the glass transition temperature of the interfacial layer increases with reducing the pore size. This phenomenon has been previously discussed in the literature.[2,4,42,43,49,52,56] Table 2 shows temperatures at which we observed the departure of the $\tau_\alpha(T)$ from the bulk dependence for PMPS 2.5 k confined in AAO nanopores with different pore sizes (20, 60, 100, 200 nm). Based on the literature findings, we can use these values to estimate vitrification temperatures of the interfacial layer as determined typically from the calorimetric studies.

In Figure 6a, we present segmental relaxation times for PMPS 2.5 k confined in nanopores with different pore sizes (20, 60, 100, and 200 nm) determined at the initial and the final stage of the annealing process carried out at the same temperature, T_{ANN} = 241 K. Here, the results of the pore size-controlled experiments are plotted as a function of the reduced temperature. As illustrated, the distance from $T_{g\_interface}$ affects the time necessary to recover the bulk relaxation time. The same annealing temperature for different pores sizes does not imply the same value of the reduced temperature. The results also indicate that during annealing experiments at T_{ANN} = 241 K, reducing the pore size causes the distance from the $T_{g\_interface}$ to increase. As we have mentioned earlier, this is related to the increase in the temperature of the vitrification of the interfacial layer. More importantly, it should also be noted that at T_{ANN} = 241 K, for each pore size, we were able to recover the bulk polymer relaxation time.

The analysis of the changes in the segmental relaxation time during the prolonged annealing allowed us to estimate the characteristic annealing time (τ_{ANN}). The literature data show that the equilibration phenomena under confinement cannot be correlated only with the changes in the mobility of segments during time experiments.[28] On the other hand, for confined PMPS 27.8 k, the relationship between equilibration kinetics and the viscous flow rate through the nanometer-sized capillary was also observed. For this reason, it was proposed that the viscous flow eventually helps to eliminate confinement effects seen in faster segmental dynamics. The characteristic time of the viscous flow rate in cylindrical channels is defined as $\tau_{flow} \propto (l/$

https://dx.doi.org/10.1021/acs.jpcc.0c07053
J. Phys. Chem. C 2020, 124, 22321−22330

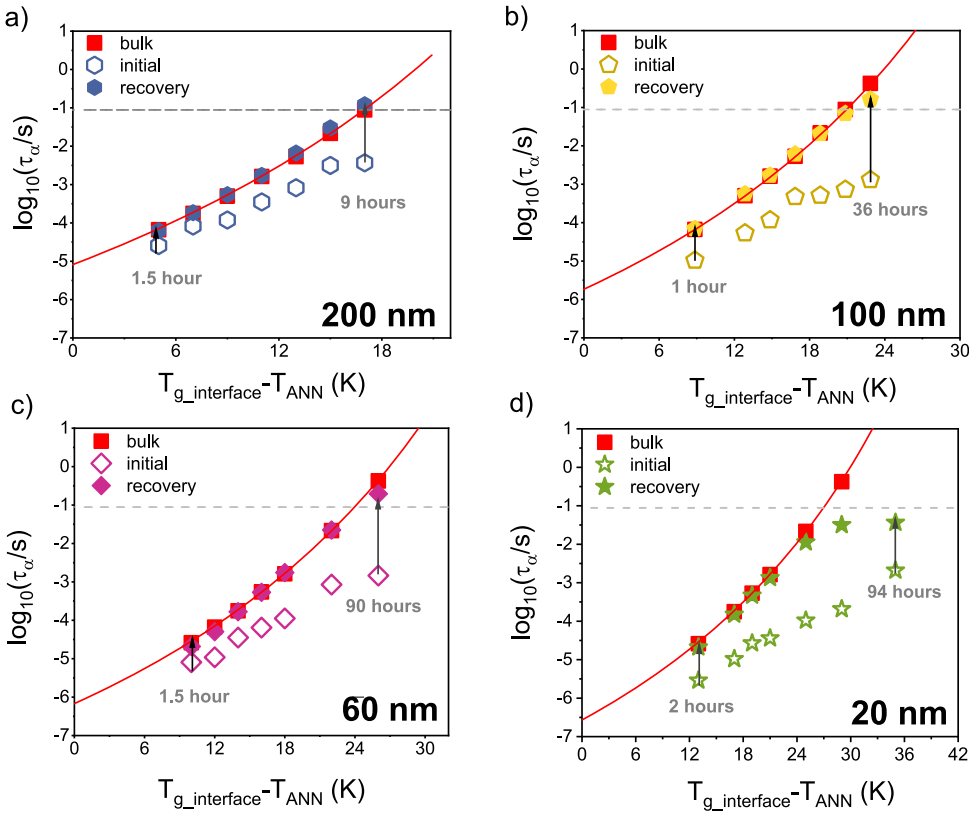

Figure 5. Segmental relaxation times plotted versus the depth of annealing upon the temperature-dependent studies for the bulk PMPS 2.5 k and confined in 20 nm (panel a), 60 nm (panel b), 100 nm (panel c), and 200 nm (panel d) AAO templates. Confinement data were collected before and after annealing at various temperatures. Solid lines are fitting of the bulk data to the VFT equation. Dashed horizontal lines indicate the same bulk value of the segmental relaxation time.

Table 2. Vitrification Temperatures of the Interfacial Layer for PMPS 2.5 k Confined in AAO Nanopores[a]

pore size (nm)	$T_{g\_interface}$ (K)
200	250
100	254
60	257
20	260

[a]Data were estimated based on DS measurements.

$r)^2\tau_\alpha$, where l is the pore length (direction of the flow) and r is the pore radius (direction perpendicular to the flow).[28] Figure 6b shows the temperature dependence of the annealing time and the calculated time of the viscous flow in the cylindrical channels for PMPS 2.5 k confined in 20 nm AAO nanopores. As shown, both the characteristic time constants differ in value. The time of the viscous flow in the cylindrical nano-channels is longer than the annealing time. In addition, in Figure 6c, we compare τ_{ANN} and τ_{flow} as a function of the pore size. These data also suggest that the difference between both the time constants for PMPS 2.5 k under nanopore-confinement occurs regardless of the pore size. Only in the case of 200 nm nanopores, $\tau_{ANN,}$ and τ_{flow} have similar values. This is in contrast to the literature data demonstrating that the obtained values of the annealing time and the characteristic time of viscous flow in the cylindrical channels for PMPS 27.8 k confined in nanopores are similar.[28] Furthermore, we have analyzed the relationship between the characteristic time constants on a log−log scale at three different temperatures (235, 239, and 241 K). Experimental data lie in a straight line with a slope of about 0.4−0.6, which suggests that as the pore diameter increases, τ_{flow} increases faster compared to τ_{ANN}.

As a next step, we have compared annealing results for PMPS 2.5 k with that collected for a high molecular weight PMPS sample (M_w = 27,800 g). The aim is to check how the length of the polymer chain affects the equilibration times in nanopores. For this purpose, in Figure 7a, we show the characteristic annealing times as a function of the pore diameter for PMPS 2.5 k and PMPS 27.8 k, determined at different temperatures but for approximately the same relaxation time (log (τ_α/s) ≅3.3). For the low molecular weight PMPS confined in AAO nanopores with different pore sizes (20, 60, 100 nm), the τ_{ANN} values are lower. For example, for the 100 nm nanopores, the time needed for bulk dynamic recovery is 3.5 and 16 h, respectively, for PM 2.5 k and PMPS 27.8 K. This fact indicates that the time needed to reach the equilibrium for the nanopore-confined PMPS 2.5 k is shorter compared to PMPS 27.8 k. For nanopores with 200 nm pore diameter, the characteristic annealing times for PMPS with different molecular weights are similar. Figure 7b presents τ_{ANN} as a function of distance from the $T_{g\_interface}$ for PMPS 2.5 k, and PMPS 27.8 k confined in 100 nm AAO nanopores (for PMPS 27.8 k embedded in 100 nm AAO nanopores $T_{g\_interface}$ = 268K[28]). As demonstrated, for the high molecular weight polymer τ_{ANN}, values are indeed greater, which confirms that shorter polymer chains under nanopore-confinement regain bulk mobility faster than longer ones.

In Figure 7c, we present the relaxation times at the initial and the final stage of annealing for PMPS 2.5 k and PMPS 27.8 k confined in 20 and 200 nm AAO nanopores. The data are plotted as a function of the reduced temperature (determined

https://dx.doi.org/10.1021/acs.jpcc.0c07053
J. Phys. Chem. C 2020, 124, 22321−22330

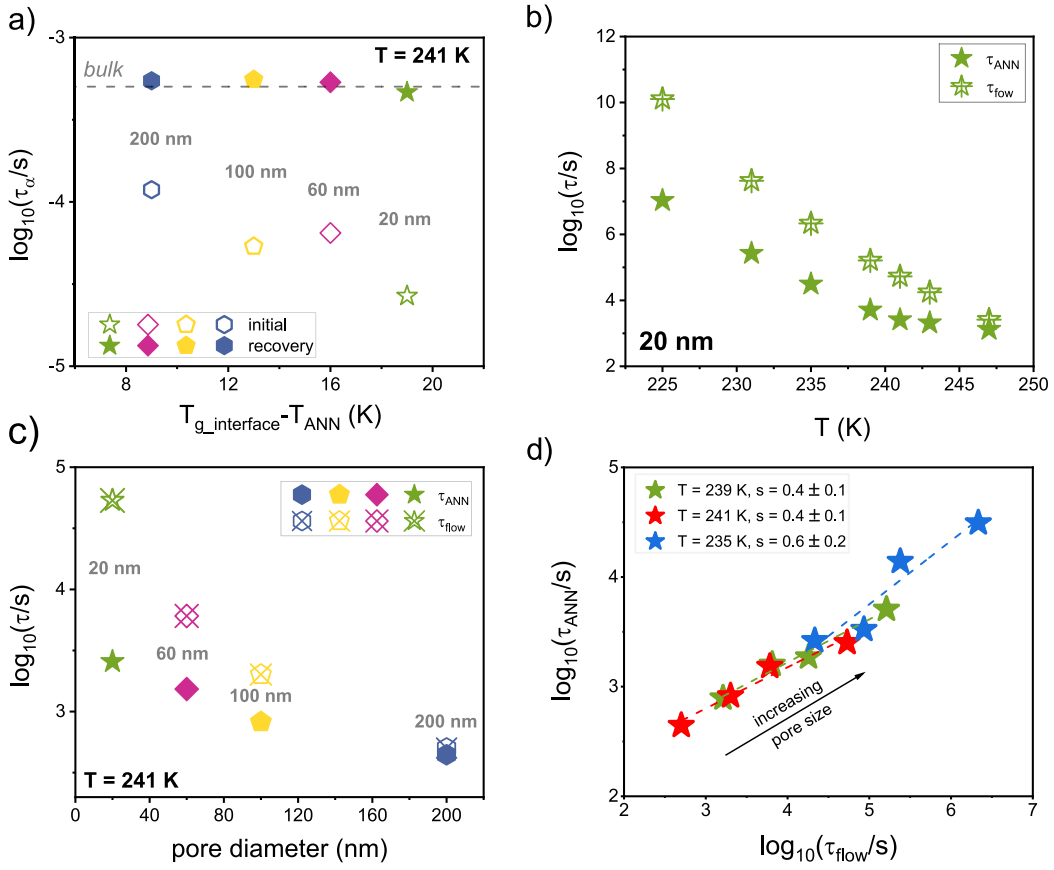

Figure 6. (a) Segmental relaxation times plotted versus the depth of annealing upon the size-dependent studies for PMPS 2.5 k measured at T_{ANN} = 241 K. Dashed horizontal line indicates the bulk value of the segmental relaxation time. (b) Comparison of the annealing time constant and the characteristic time of viscous flow in the cylindrical channels for PMPS 2.5 k in AAO nanopores of 20 nm diameter. (c) Annealing time constant and the characteristic time of viscous flow in the cylindrical channels plotted versus pore diameter for PMPS 2.5 k confined to nanopores with different pore sizes. (d) Annealing time constant versus the characteristic time of the viscous flow in the cylindrical channels for PMPS 2.5 k confined in nanopores with different pore sizes. Data were collected at three different annealing temperatures (235, 239, and 241 K). Dashed lines represent linear fits to the data.

using individual values of the $T_{g\_interface}$ for low and high molecular weight samples). As shown, for both PMPS samples confined in 200 nm, the bulk relaxation time was recovered. However, in the case of the 20 nm pore diameter, only PMPS 2.5 k regains bulk α-relaxation time. For PMPS 27.8 k confined in 20 nm nanopores, the time needed to recover the bulk behavior exceeds the time available experimentally. Thus, our results suggest that the observed differences in the equilibration time for PMPS 2.5 k and PMPS 27.8 k are due to the different polymer chains' length. It appears that a longer chain requires more time to reorganize and approach denser packing in the nanopores. A similar result was previously reported in the literature. For poly(propylene glycol) derivatives, it has been shown that for higher-molecular-weight samples, equilibration kinetics is slowed-down in nanopore-confinement.[57] For PMPS 27.8 k, experimental results suggest a coupling between the characteristic annealing time and the characteristic time of the viscous flow in the cylindrical channels (slope ~0.9).[28] In Figure 7d, we present the relationship between these time constants in the log–log scale for PMPS 2.5 k and PMPS 27.8 k. We have chosen data that correspond approximately to the same relaxation time for both molecular weights of the tested polymer. As illustrated, in the case of the low molecular weight polymer, experimental data form a line with a slope of 0.4. For the same pore size, τ_{ANN} has a smaller value compared to the value of τ_{flow}. These data show that the molecular weight of the polymer embedded in nanopores can also affect the relationship between the characteristic annealing time and the viscous flow rate in the cylindrical nanochannels.

Finally, Figure 8 shows a comparison of the distribution of α-relaxation times for PMPS 2.5 k and PMPS 27.8 k in bulk and confined in 100 nm AAO nanopores. Spectra for confined PMPS of different molecular weights refer to prolonged annealing of samples that regain τ_α characteristic for bulk samples. Since T_g for the polymer material depends on its molecular weight, the dielectric loss spectra were recorded at different temperatures but for approximately the same segmental relaxation time ($\log_{10}(\tau_\alpha/s) \cong -3.3$). As demonstrated, the α-loss peak for the low molecular weight PMPS in 100 nm pores is slightly broader than the distribution of relaxation time for the confined polymer with a higher molecular weight. The β_{KWW} parameter values in 100 nm pores are 0.31 and 0.36 for PMPS 2.5 k and PMPs 27.8 k, respectively. This indicates that after the equilibration process, the dynamics of the low molecular weight tested polymer embedded in cylindrical nanopores has a slightly more heterogeneous character than the dynamics of the high molecular weight sample. It should be added that the difference in the distribution of relaxation time is also visible for bulk samples. The shape of the α-loss peak for PMPS 2.5 k is broader

https://dx.doi.org/10.1021/acs.jpcc.0c07053
J. Phys. Chem. C 2020, 124, 22321−22330

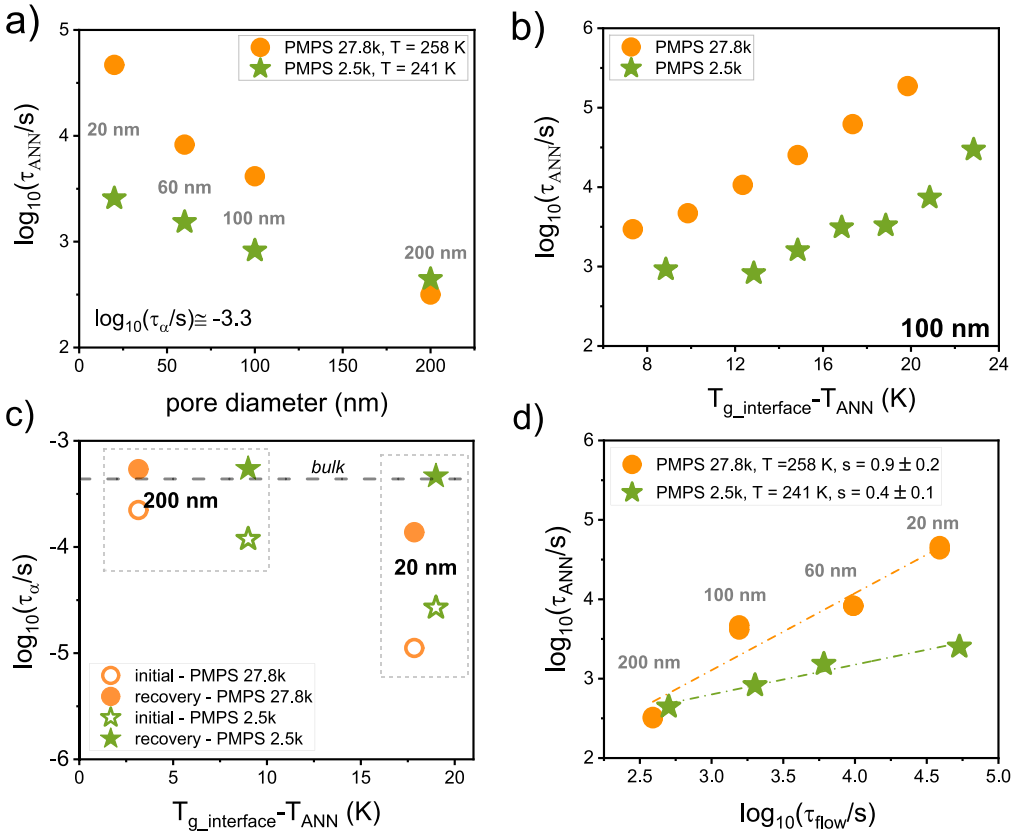

Figure 7. (a) Comparison of annealing time constants for PMPS 2.5 k and PMPS 27.8 k confined in AAO templates of different pore sizes taken at different temperatures but for approximately the same segmental relaxation time. (b) Annealing time constant plotted versus the depth of annealing upon the temperature-dependent studies for PMPS 2.5 k and PMPS 27.8 k confined in the 100 nm AAO templates. (c) Segmental relaxation times plotted versus the depth of the annealing upon the size-dependent studies measured for PMPS 2.5 k and PMPS 27.8 k confined in 200 and 20 nm AAO nanopores. Data for both samples are characterized by approximately the same segmental relaxation time. Dashed horizontal line indicates the bulk value of the segmental time. (d) Annealing time constant versus the characteristic time of viscous flow in cylindrical channels for PMPS 2.5 k and PMPS 27.8 k confined in nanopores with different pore sizes. Data were recorded for approximately the same segmental relaxation time. Dashed lines represent linear fits to the data. Data for PMPS 27.8 k were taken from the literature.[28]

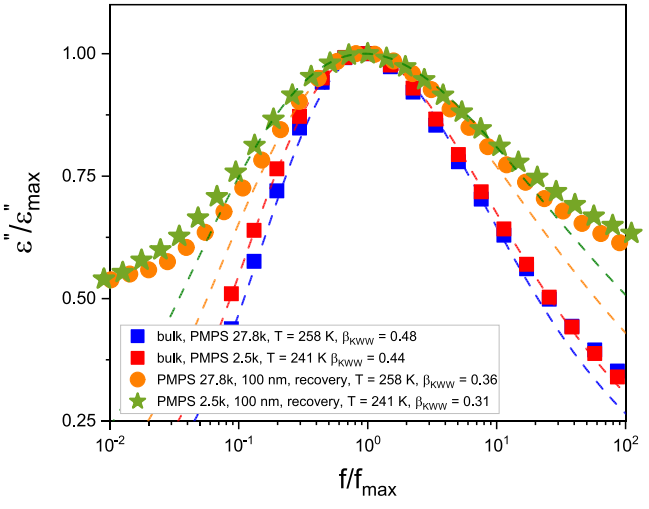

Figure 8. Comparison of the normalized dielectric loss spectra for PMPS 2.5 k and PMPS 27.8 k in bulk and confined to 100 nm AOO nanopores. Spectra for confined polymers referred to prolonged annealing of samples and were recorded at different temperatures but for approximately the same segmental relaxation time ($\log_{10}(\tau_\alpha/s) \cong -3.3$). Dashed lines are fits to the KWW function.

than that for PMPS 27.8 k, which is consistent with the literature data.[38]

SUMMARY AND CONCLUSIONS

In this work, by employing dielectric spectroscopy, we have studied the effect of molecular weight on equilibration phenomena of a nanopore-confined polymer. For this purpose, we have used poly(phenylmethyl siloxane with low (M_w = 2530 g/mol) and high (M_w = 27,800 g/mol) molecular weight. We have shown that the faster dynamics observed in a confined geometry realized by cylindrical nanopores reveals a pronounced nonequilibrium nature but has a limited lifetime. Annealing below the glass transition temperature of the interfacial layer allows one to regain the bulk mobility. The nanopore-confined polymer needs sufficient time to rearrange and approach the equilibrium conformation of the polymer chains. In addition, we have found out that the annealing temperature and the pore size influence the equilibration time. The larger the temperature jump below $T_{g\_interface}$, the more the time needed to eliminate the confinement effect and approach the bulk-like dynamics. Our results are consistent with the data reported for nanopores and thin films.[20−22,24,28]

Moreover, experimental data analysis has revealed that the molecular weight of the polymer affects the equilibration phenomena in the nanopores. We have demonstrated that low-

https://dx.doi.org/10.1021/acs.jpcc.0c07053
J. Phys. Chem. C 2020, 124, 22321−22330

molecular-weight PMPS recovers bulk properties more effectively than the high-molecular-weight one. This fact suggests that a longer polymer chain needs more time to rearrange and attain a more densely packed alignment of the polymer chains in a nanoconfined geometry. It can also be added that PMPS with two considered molecular weights have a very similar sensitivity to density effects. The value of the pressure coefficient of the glass-transition temperature, dT_g/dP, is 0.28 and 0.29 K/MPa for PMPS 2.5 k and PMPS 27.8 k, respectively. This suggests that, in both cases, the sensitivity of the tested samples to density frustrations is comparable.[38]

We have also shown that the molecular weight of the nanopore-confined polymer can influence the relationship between the equilibration kinetics in nanopores and the viscous flow rate in the cylindrical nanochannels. Literature data demonstrate the coupling between τ_{ANN} and τ_{flow} for high molecular weight PMPS. In that case, both characteristic time constants have similar values. However, for PMPS 2.5 k, the characteristic time of the viscous flow in the cylindrical channels is longer than the characteristic annealing time. Therefore, it is evident that the confinement effects seen as faster segmental relaxation times are not solely released by the viscous flow.

Summarizing, our research shows that not only the pore size and the annealing temperature but also the molecular weight of the tested polymer have a significant impact on the equilibrium phenomena under nanopore-confinement. The molecular weight also affects the time necessary for rearrangement and approaching more dense packing of the polymer chains in nanopores, as well as the relationship between τ_{ANN} and τ_{flow}. Thus, the results of this study provide valuable information to better understand complex nonequilibrium phenomena of polymer systems in a confined geometry, which is vital for their applications in different fields.

AUTHOR INFORMATION

Corresponding Authors

Katarzyna Chat − *Institute of Physics, University of Silesia, 41-500 Chorzow, Poland; Silesian Center for Education and Interdisciplinary Research (SMCEBI), 41-500 Chorzow, Poland;* orcid.org/0000-0002-6972-2859; Email: kchat@us.edu.pl

Karolina Adrjanowicz − *Institute of Physics, University of Silesia, 41-500 Chorzow, Poland; Silesian Center for Education and Interdisciplinary Research (SMCEBI), 41-500 Chorzow, Poland;* orcid.org/0000-0003-0212-5010; Email: kadrjano@us.edu.pl

Complete contact information is available at: https://pubs.acs.org/10.1021/acs.jpcc.0c07053

Notes

The authors declare no competing financial interest.

ACKNOWLEDGMENTS

The authors acknowledge financial assistance from the National Science Centre (Poland) within the Project OPUS 14 nr. UMO-2017/27/B/ST3/00402.

REFERENCES

(1) Richert, R. Dynamics of Nanoconfined Supercooled Liquids. *Annu. Rev. Phys. Chem.* **2011**, *62*, 65−84.

(2) Adrjanowicz, K.; Kaminski, K.; Tarnacka, M.; Szklarz, G.; Paluch, M. Predicting Nanoscale Dynamics of a Glass-Forming Liquid from Its Macroscopic Bulk Behavior and Vice Versa. *J. Phys. Chem. Lett.* **2017**, *8*, 696−702.

(3) Adrjanowicz, K.; Kaminski, K.; Koperwas, K.; Paluch, M. Negative Pressure Vitrification of the Isochorically Confined Liquid in Nanopores. *Phys. Rev. Lett.* **2015**, *115*, 265702.

(4) Adrjanowicz, K.; Kolodziejczyk, K.; Kipnusu, W. K.; Tarnacka, M.; Mapesa, E. U.; Kaminska, E.; Pawlus, S.; Kaminski, K.; Paluch, M. Decoupling between the Interfacial and Core Molecular Dynamics of Salol in 2D Confinement. *J. Phys. Chem. C* **2015**, *119*, 14366−14374.

(5) Adrjanowicz, K.; Winkler, R.; Chat, K.; Duarte, D. M.; Tu, W.; Unni, A. B.; Paluch, M.; Ngai, K. L. Study of Increasing Pressure and Nanopore Confinement Effect on the Segmental, Chain, and Secondary Dynamics of Poly(Methylphenylsiloxane). *Macromolecules* **2019**, *52*, 3763−3774.

(6) Adrjanowicz, K.; Winkler, R.; Dzienia, A.; Paluch, M.; Napolitano, S. Connecting 1D and 2D Confined Polymer Dynamics to Its Bulk Behavior via Density Scaling. *ACS Macro Lett.* **2019**, *8*, 304−309.

(7) Huwe, A.; Kremer, F.; Behrens, P.; Schwieger, W. Dielectric Investigations of the Dynamic Glass Transition in Nanopores; Molecular Dynamics in Confining Space: From the Single Molecule to the Liquid State. *Phys. Rev. Lett.* **1999**, *82*, 2338−2341.

(8) Napolitano, S.; Glynos, E.; Tito, N. B. Glass Transition of Polymers in Bulk, Confined Geometries, and near Interfaces. *Reports Prog. Phys.* **2017**, *80*, No. 036602.

(9) Kremer, F. *Dynamics in Geometrical Confinement*; Springer: Cham, 2014.

(10) Pissis, P.; Daoukaki-Diamanti, D.; Apekis, L.; Christodoulides, C. The Glass Transition in Confined Liquids. *J. Phys. Condens. Matter* **1994**, *6*, L325−L328.

(11) Keddie, J. L.; Jones, R. A. L.; Cory, R. A. Interface and Surface Effects on the Glass-Transition Temperature in Thin Polymer Films. *Faraday Discuss.* **1994**, *98*, 219.

(12) Jackson, C. L.; McKenna, G. B. The Glass Transition of Organic Liquids Confined to Small Pores. *J. Non-Cryst. Solids* **1991**, *131-133*, 221−224.

(13) Rittigstein, P.; Torkelson, J. M. Polymer-Nanoparticle Interfacial Interactions in Polymer Nanocomposites: Confinement Effects on Glass Transition Temperature and Suppression of Physical Aging. *J. Polym. Sci. Part B Polym. Phys.* **2006**, *44*, 2935−2943.

(14) Ellison, C. J.; Torkelson, J. M. The Distribution of Glass-Transition Temperatures in Nanoscopically Confined Glass Formers. *Nat. Mater.* **2003**, *2*, 695−700.

(15) Jackson, C. L.; McKenna, G. B. Vitrification and Crystallization of Organic Liquids Confined to Nanoscale Pores. *Chem. Mater.* **1996**, *8*, 2128−2137.

(16) Fukao, K. Dynamics in Thin Polymer Films by Dielectric Spectroscopy. *Eur. Phys. J. E: Soft Matter Biol. Phys.* **2003**, *12*, 119−125.

(17) Beena Unni, A.; Chat, K.; Duarte, D. M.; Wojtyniak, M.; Geppert-Rybczyńska, M.; Kubacki, J.; Wrzalik, R.; Richert, R.; Adrjanowicz, K. Experimental Evidence on the Effect of Substrate Roughness on Segmental Dynamics of Confined Polymer Films. *Polymer* **2020**, *199*, 122501.

(18) Kipnusu, W. K.; Elmahdy, M. M.; Elsayed, M.; Krause-Rehberg, R.; Kremer, F. Counterbalance between Surface and Confinement Effects As Studied for Amino-Terminated Poly(Propylene Glycol) Constraint in Silica Nanopores. *Macromolecules* **2019**, *52*, 1864−1873.

(19) Talik, A.; Tarnacka, M.; Grudzka-Flak, I.; Maksym, P.; Geppert-Rybczynska, M.; Wolnica, K.; Kaminska, E.; Kaminski, K.; Paluch, M. The Role of Interfacial Energy and Specific Interactions on the Behavior of Poly(Propylene Glycol) Derivatives under 2D Confinement. *Macromolecules* **2018**, *51*, 4840−4852.

(20) Serghei, A.; Kremer, F. Metastable States of Glassy Dynamics, Possibly Mimicking Confinement-Effects in Thin Polymer Films. *Macromol. Chem. Phys.* **2008**, *209*, 810−817.

(21) Panagopoulou, A.; Napolitano, S. Irreversible Adsorption Governs the Equilibration of Thin Polymer Films. *Phys. Rev. Lett.* **2017**, *119*, No. 097801.

(22) Nguyen, H. K.; Labardi, M.; Capaccioli, S.; Lucchesi, M.; Rolla, P.; Prevosto, D. Interfacial and Annealing Effects on Primary α-

Relaxation of Ultrathin Polymer Films Investigated at Nanoscale. *Macromolecules* **2012**, *45*, 2138−2144.
(23) Nguyen, H. K.; Labardi, M.; Lucchesi, M.; Rolla, P.; Prevosto, D. Plasticization in Ultrathin Polymer Films: The Role of Supporting Substrate and Annealing. *Macromolecules* **2013**, *46*, 555−561.
(24) Napolitano, S. *Non-Equilibrium Phenomena in Confined Soft Matter: Irreversible Adsorption, Physical Aging and Glass Transition at the Nanoscale*; Springer, 2015.
(25) Napolitano, S.; Wübbenhorst, M. The Lifetime of the Deviations from Bulk Behaviour in Polymers Confined at the Nanoscale. *Nat. Commun.* **2011**, *2*, 260.
(26) Rotella, C.; Napolitano, S.; Vandendriessche, S.; Valev, V. K.; Verbiest, T.; Larkowska, M.; Kucharski, S.; Wübbenhorst, M. Adsorption Kinetics of Ultrathin Polymer Films in the Melt Probed by Dielectric Spectroscopy and Second-Harmonic Generation. *Langmuir* **2011**, *27*, 13533−13538.
(27) Rotella, C.; Wübbenhorst, M.; Napolitano, S. Probing Interfacial Mobility Profiles via the Impact of Nanoscopic Confinement on the Strength of the Dynamic Glass Transition. *Soft Matter* **2011**, *7*, 5260−5266.
(28) Adrjanowicz, K.; Paluch, M. Discharge of the Nanopore Confinement Effect on the Glass Transition Dynamics via Viscous Flow. *Phys. Rev. Lett.* **2019**, *122*, 176101.
(29) Tarnacka, M.; Dulski, M.; Geppert-Rybczyńska, M.; Talik, A.; Kamińska, E.; Kamiński, K.; Paluch, M. Variation in the Molecular Dynamics of DGEBA Confined within AAO Templates above and below the Glass-Transition Temperature. *J. Phys. Chem. C* **2018**, *122*, 28033−28044.
(30) Winkler, R.; Tu, W.; Laskowski, L.; Adrjanowicz, K. Effect of Surface Chemistry on the Glass-Transition Dynamics of Poly(Phenyl Methyl Siloxane) Confined in Alumina Nanopores. *Langmuir* **2020**, *36*, 7553−7565.
(31) Napolitano, S.; Rotella, C.; Wübbenhorst, M. Can Thickness and Interfacial Interactions Univocally Determine the Behavior of Polymers Confined at the Nanoscale? *ACS Macro Lett.* **2012**, *1*, 1189−1193.
(32) Napolitano, S.; Capponi, S.; Vanroy, B. Glassy Dynamics of Soft Matter under 1D Confinement: How Irreversible Adsorption Affects Molecular Packing, Mobility Gradients and Orientational Polarization in Thin Films. *Eur. Phys. J. E: Soft Matter Biol. Phys.* **2013**, *36*, 61.
(33) Perez-De-Eulate, N. G.; Sferrazza, M.; Cangialosi, D.; Napolitano, S. Irreversible Adsorption Erases the Free Surface Effect on the T g of Supported Films of Poly(4- Tert -Butylstyrene). *ACS Macro Lett.* **2017**, *6*, 354−358.
(34) Napolitano, S.; Sferrazza, M. How Irreversible Adsorption Affects Interfacial Properties of Polymers. *Adv. Colloid Interface Sci.* **2017**, *247*, 172−177.
(35) Tarnacka, M.; Kaminski, K.; Mapesa, E. U.; Kaminska, E.; Paluch, M. Studies on the Temperature and Time Induced Variation in the Segmental and Chain Dynamics in Poly(Propylene Glycol) Confined at the Nanoscale. *Macromolecules* **2016**, *49*, 6678−6686.
(36) Tarnacka, M.; Madejczyk, O.; Kaminski, K.; Paluch, M. Time and Temperature as Key Parameters Controlling Dynamics and Properties of Spatially Restricted Polymers. *Macromolecules* **2017**, *50*, 5188−5193.
(37) Tarnacka, M.; Kaminska, E.; Kaminski, K.; Roland, C. M.; Paluch, M. Interplay between Core and Interfacial Mobility and Its Impact on the Measured Glass Transition: Dielectric and Calorimetric Studies. *J. Phys. Chem. C* **2016**, *120*, 7373−7380.
(38) Tu, W.; Ngai, K. L.; Paluch, M.; Adrjanowicz, K. Dielectric Study on the Well-Resolved Sub-Rouse and JG β-Relaxations of Poly(Methylphenylsiloxane) at Ambient and Elevated Pressures. *Macromolecules* **2020**, *53*, 1706−1715.
(39) Alexandris, S.; Papadopoulos, P.; Sakellariou, G.; Steinhart, M.; Butt, H.-J. J.; Floudas, G. Interfacial Energy and Glass Temperature of Polymers Confined to Nanoporous Alumina. *Macromolecules* **2016**, *49*, 7400−7414.
(40) Richert, R. Comment on "Hidden Slow Dynamics in Water". *Phys. Rev. Lett.* **2010**, *104*, 249801.
(41) Paluch, M.; Pawlus, S.; Kaminski, K. Comment on "Slow Debye-Type Peak Observed in the Dielectric Response of Polyalcohols" [J. Chem. Phys. 132, 044504 (2010)]. *J. Chem. Phys.* **2011**, *134*, No. 037101.
(42) Szklarz, G.; Adrjanowicz, K.; Tarnacka, M.; Pionteck, J.; Paluch, M. Confinement-Induced Changes in the Glassy Dynamics and Crystallization Behavior of Supercooled Fenofibrate. *J. Phys. Chem. C* **2018**, *122*, 1384−1395.
(43) Chat, K.; Tu, W.; Laskowski, L.; Adrjanowicz, K. Effect of Surface Modification on the Glass Transition Dynamics of Highly Polar Molecular Liquid S-Methoxy-PC Confined in Anodic Aluminum Oxide Nanopores. *J. Phys. Chem. C* **2019**, *123*, 13365−13376.
(44) Havriliak, S.; Negami, S. A Complex Plane Representation of Dielectric and Mechanical Relaxation Processes in Some Polymers. *Polymer* **1967**, *8*, 161−210.
(45) Vogel, H. The Law of the Relation between the Viscosity of Liquids and the Temperature. *Phys. Z.* **1921**, *22*, 645−646.
(46) Fulcher, G. S. Analysis of Recent Measurements of the Viscosity of Glasses. *J. Am. Ceram. Soc.* **1925**, *8*, 339−355.
(47) Tammann, G.; Hesse, W. Die Abhängigkeit Der Viscosität von Der Temperatur Bie Unterkühlten Flüssigkeiten. *Z. Anorg. Allg. Chem.* **1926**, *156*, 245−257.
(48) Adrjanowicz, K.; Szklarz, G.; Koperwas, K.; Paluch, M. Comparison of High Pressure and Nanoscale Confinement Effects on Crystallization of the Molecular Glass-Forming Liquid, Dimethyl Phthalate. *Phys. Chem. Chem. Phys.* **2017**, *19*, 14366−14375.
(49) Chat, K.; Tu, W.; Beena Unni, A.; Geppert-Rybczyńska, M.; Adrjanowicz, K. Study on the Glass Transition Dynamics and Crystallization Kinetics of Molecular Liquid, Dimethyl Phthalate, Confined in Anodized Aluminum Oxide (AAO) Nanopores with Atomic Layer Deposition (ALD) Coatings. *J. Mol. Liq.* **2020**, *311*, 113296.
(50) Talik, A.; Tarnacka, M.; Geppert-Rybczynska, M.; Minecka, A.; Kaminska, E.; Kaminski, K.; Paluch, M. Impact of the Interfacial Energy and Density Fluctuations on the Shift of the Glass-Transition Temperature of Liquids Confined in Pores. *J. Phys. Chem. C* **2019**, *123*, 5549−5556.
(51) Talik, A.; Tarnacka, M.; Wojtyniak, M.; Kaminska, E.; Kaminski, K.; Paluch, M. The Influence of the Nanocurvature on the Surface Interactions and Molecular Dynamics of Model Liquid Confined in Cylindrical Pores. *J. Mol. Liq.* **2020**, *298*, 111973.
(52) Park, J.-Y.; McKenna, G. B. Size and Confinement Effects on the Glass Transition Behavior of Polystyrene/o-Terphenyl Polymer Solutions. *Phys. Rev. B* **2000**, *61*, 6667−6676.
(53) Kohlrausch, R. Nachtrag Uber Die Elastische Nachwirkung Beim Cocon Und Glasfaden. *Ann. Phys.* **1847**, *72*, 7.
(54) Williams, G.; Watts, D. C. Non-Symmetrical Dielectric Relaxation Behaviour Arising from a Simple Empirical Decay Function. *Trans. Faraday Soc.* **1970**, *66*, 80−85.
(55) Alvarez, F.; Alegra, A.; Colmenero, J. Relationship between the Time-Domain Kohlrausch-Williams-Watts and Frequency-Domain Havriliak-Negami Relaxation Functions. *Phys. Rev. B* **1991**, *44*, 7306−7312.
(56) Li, L.; Zhou, D.; Huang, D.; Xue, G. Double Glass Transition Temperatures of Poly(Methyl Methacrylate) Confined in Alumina Nanotube Templates. *Macromolecules* **2014**, *47*, 297−303.
(57) Tarnacka, M.; Talik, A.; Kamińska, E.; Geppert-Rybczyńska, M.; Kaminski, K.; Paluch, M. The Impact of Molecular Weight on the Behavior of Poly(Propylene Glycol) Derivatives Confined within Alumina Templates. *Macromolecules* **2019**, *52*, 3516−3529.

https://dx.doi.org/10.1021/acs.jpcc.0c07053
J. Phys. Chem. C 2020, 124, 22321−22330